R. & M. No. 3115
(19,930)
A.R.C. Technical Report

MINISTRY OF SUPPLY

AERONAUTICAL RESEARCH COUNCIL
REPORTS AND MEMORANDA

The Influence of Aerodynamic Heating on the Flexural Rigidity of a Thin Wing

By

E. H. MANSFIELD, Sc.D.

LONDON: HER MAJESTY'S STATIONERY OFFICE
1959
PRICE 9*s*. 6*d*. NET

The Influence of Aerodynamic Heating on the Flexural Rigidity of a Thin Wing

By

E. H. MANSFIELD, Sc.D.

COMMUNICATED BY THE DIRECTOR-GENERAL OF SCIENTIFIC RESEARCH (AIR), MINISTRY OF SUPPLY

Reports and Memoranda No. 3115*

September, 1957

Summary.—This report considers the loss of flexural rigidity of a thin wing due to the presence of middle-surface stresses resulting from aerodynamic heating. The spanwise properties of the wing are assumed constant but the wing section is arbitrary. The loss of flexural rigidity is comparable with the corresponding loss of torsional rigidity.

1. *Introduction.*—One of the problems arising from the aerodynamic heating of a wing is that thermal stresses may reduce the overall stiffness of the wing.

If a thin solid wing is accelerated to a high Mach number its temperature will eventually reach the saturation temperature appropriate to that Mach number. Before this steady state occurs, however, there is a transient period during which the thinner parts of the wing, due mainly to their smaller heat capacity, attain a higher temperature than the thicker parts of the wing. These chordwise variations of temperature give rise to a thermal stress distribution which, away from any end effect, is characterised by spanwise compressive stresses at the leading and trailing edges and equilibrating tensile stresses at the mid-chord. If the wing remains perfectly flat these middle surface stresses are completely self-equilibrating ; but if the wing is twisted the middle surface stresses have a resultant torque acting in the same sense as the twist, and this results in an effective reduction of the torsional rigidity[1, 2, 3, 4, 5, 6].

The present report is concerned with the loss of flexural rigidity due to these middle surface stresses. If the wing bends, its cross-section distorts for two reasons : first, because of the Poisson's ratio effect, and second, because of the radial component of the middle surface stresses. The middle surface stresses tend to relieve themselves as in the Brazier effect[7], the elements in compression expanding by moving radially further away from the centre of curvature and the elements in tension contracting by moving radially towards the centre of curvature.

These two components of the distortion of the cross-section are, roughly speaking, additive in the sense that elements containing middle surface stresses of the same sign move away from the neutral axis in the same direction. Because of this distortion the middle surface stresses now have a resultant moment acting in the same sense as the applied moment, and this results in an effective reduction of the flexural rigidity.

* R.A.E. Report Structures 229, received 28th February, 1958.

The main body of the report considers the flexural behaviour of a thin solid wing of infinite aspect ratio with a given chordwise distribution of spanwise middle surface stresses. How these middle surface stresses arise due to aerodynamic heating is discussed briefly in Appendix I and the influence of end effects in a wing of finite aspect ratio is considered in Appendix II. The flexural rigidity of a built-up wing is considered in Appendix III.

2. *Method of Analysis in Large-Deflection Theory.*—In order to determine the flexural rigidity of the wing it is first necessary to determine the chordwise variation of distortion of the wing due to a given spanwise curvature. The differential equation which governs this distortion is found in Section 2.1. The boundary conditions appropriate to this differential equation, and hence expressions for the spanwise bending moment and the flexural rigidity are found in Section 2.2. The complete large-deflection behaviour of a strip of constant thickness with a parabolic chordwise variation of middle-surface stresses is considered in Appendix IV. A small-deflection theory for wings of arbitrary chordwise thickness variation is presented in Section 3.

2.1. *Derivation of the Differential Equation.*—The chordwise variation of the distortion of the wing may be found most conveniently by variational methods. We shall consider a long solid wing with arbitrary chordwise thickness variation, bent into the form of a 'near cylinder' of radius R. The distortion of the wing is then of the form

$$w(x,y) = \frac{y^2}{2R} + w(x) \quad \ldots \quad (1)$$

and $w(x)$, hereafter referred to simply as w, is such that the total strain energy of the wing is a minimum.

The strain energy due to strains in the middle surface of the wing will now be determined. A displacement w from the cylindrical shape, positive if directed toward the centre of the cylinder, reduces the circumferential strain by an amount w/R. The circumferential strain is therefore given by

$$\varepsilon = \bar{\varepsilon} - \frac{w}{R}. \quad \ldots \quad (2)$$

As there are no chordwise middle-surface stresses, the strain energy per unit length due to the middle-surface strains is given by

$$V_m = \frac{1}{2}\int_{-a/2}^{+a/2} Et\left(\bar{\varepsilon} - \frac{w}{R}\right)^2 dx\,. \quad \ldots \quad (3)$$

The strain energy per unit length due to flexure is given by[8]

$$\begin{aligned} V_f &= \frac{1}{2}\int_{-a/2}^{+a/2} D\left[\{\nabla^2 w(x,y)\}^2 - 2(1-\nu)\frac{\partial^2 w(x,y)}{\partial x^2}\frac{\partial^2 w(x,y)}{\partial y^2}\right] dx \\ &= \frac{1}{2}\int_{-a/2}^{+a/2} D\left\{\left(\frac{d^2 w}{dx^2}\right)^2 + \frac{2\nu}{R}\frac{d^2 w}{dx^2} + \frac{1}{R^2}\right\} dx \quad \ldots \quad (4) \end{aligned}$$

by virtue of equation (1).

The total strain energy per unit length is the sum of these two and the condition that this is a minimum with respect to w requires[9] w to satisfy the following differential equation

$$\frac{d^2}{dx^2}\left\{D\left(\frac{d^2 w}{dx^2} + \frac{\nu}{R}\right)\right\} - \frac{Et}{R}\left(\bar{\varepsilon} - \frac{w}{R}\right) = 0\,. \quad \ldots \quad (5)$$

At this stage it is convenient to introduce the following non-dimensional forms :

$$\left.\begin{aligned}
\xi &= 2x/a \\
\eta &= 2y/a \\
t^* &= Et/E_0t_0 \\
D^* &= D/D_0 \\
&= (t^*)^3 \text{ , if } E \text{ does not vary} \\
\mu^4 &= \frac{3(1-\nu^2)a^4}{16R^2t_0^{\,2}} \\
w^*(\xi, \eta) &= \left(\frac{4R}{a^2}\right) w(x,y) \text{ ,} \\
&\text{so that from equation (1)} \\
\frac{\partial^2 w^*(\xi, \eta)}{\partial \eta^2} &= 1 \text{ ,} \\
w^* &= \left(\frac{4R}{a^2}\right) w \\
\Sigma &= \left(\frac{a}{t_0}\right)^2 \left[(\bar{\varepsilon})_{x=0} - \tfrac{1}{2}\{(\bar{\varepsilon})_{x=a/2} + (\bar{\varepsilon})_{x=-a/2}\}\right] \\
&= \text{temperature-strain parameter} \\
\varepsilon^* &= \bar{\varepsilon} \Big/ \left[(\bar{\varepsilon})_{x=0} - \tfrac{1}{2}\{(\bar{\varepsilon})_{x=a/2} + (\bar{\varepsilon})_{x=-a/2}\}\right] \text{ ,} \\
&\text{so that} \\
\bar{\varepsilon} &= \Sigma \varepsilon^* \left(\frac{t_0}{a}\right)^2
\end{aligned}\right\} \quad \ldots \quad \ldots \quad \ldots \quad (6)$$

It should be noted that as x varies from $-\frac{1}{2}a$ through zero to $+\frac{1}{2}a$, ξ varies from -1 through zero to $+1$ and t^* and D^* vary (for a wing section) from zero through 1 to zero. For a heated wing, Σ is proportional to the difference between the average temperature of the leading and trailing edges and the mid-chord temperature.

In non-dimensional form, equation (5) becomes

$$\frac{d^2}{d\xi^2}\left\{D^*\left(\frac{d^2w^*}{d\xi^2} + \nu\right)\right\} + 4\mu^4 t^* w^* = 3(1-\nu^2)\Sigma t^* \varepsilon^* \text{ .} \quad \ldots \quad \ldots \quad \ldots \quad (7)$$

2.2. *Boundary Conditions*.—The differential equation above, which governs the chordwise variation of the wing distortion, is of the fourth order and the four boundary conditions which are required to complete the integration of the equation express the fact that the leading and trailing edges are free.

There are also restrictions on the possible forms of ε arising from the fact that the middle-surface stresses have no spanwise resultants ; to achieve this spanwise equilibrium, the wing may expand and assume a curvature in its own plane. The spanwise equilibrium is considered in Section 2.2.2.

The total moment acting on the wing section depends on the spanwise radius of curvature and on the chordwise distortion. A simple expression for the total moment is obtained in Section 2.2.3.

2.2.1. *Equilibrium normal to the strip.*—The edges of the strip are free and this leads to the following boundary conditions :

$$\left[D^*\left(\frac{d^2w^*}{d\xi^2} + \nu\right)\right]_{\xi=\pm 1} = 0\,, \quad \ldots \quad (8)$$

$$\left[\frac{d}{d\xi}\left\{D^*\left(\frac{d^2w^*}{d\xi^2} + \nu\right)\right\}\right]_{\xi=\pm 1} = 0\,. \quad \ldots \quad (9)$$

2.2.2. *Spanwise, or circumferential, equilibrium.*—The middle-surface forces have no resultant in the original plane of the strip. Thus by resolving and taking moments we have

$$\int_{-a/2}^{+a/2} E\varepsilon t\, dx = 0\,, \quad \ldots \quad (10)$$

$$\int_{-a/2}^{+a/2} xE\varepsilon t\, dx = 0\,, \quad \ldots \quad (11)$$

where ε is given by equation (2).

Equations (10) and (11) are valid for any value of R and are therefore valid when ε is replaced by $\bar{\varepsilon}$ or, by virtue of equation (2), w/R. In non-dimensional form equations (10) and (11) then become

$$\int_{-1}^{+1} \varepsilon^*t^*\, d\xi = 0\,, \quad \ldots \quad (12)$$

$$\int_{-1}^{+1} \xi\varepsilon^*t^*\, d\xi = 0\,, \quad \ldots \quad (13)$$

and

$$\int_{-1}^{+1} w^*t^*\, d\xi = 0\,, \quad \ldots \quad (14)$$

$$\int_{-1}^{+1} \xi w^*t^*\, d\xi = 0\,. \quad \ldots \quad (15)$$

It would appear at first sight that equations (14) and (15) represent two further boundary conditions for w^* in addition to the four given in Section 2.2.1, but this is not so, for they may be obtained from them by integrating equation (7) and using the equilibrium conditions embodied in equations (12) and (13).

It should be noted that for a heated wing with a chordwise temperature distribution $T(x)$,

$$\bar{\varepsilon} = A_1 + A_2x - \alpha T(x) \quad \ldots \quad (16)$$

and equations (12) and (13) enable the constants A_1 and A_2 to be determined.

2.2.3. *Total moment acting on cross-section of wing.*—The moment due to flexure about the middle surface of the wing is given by

$$M_f = \int_{-a/2}^{+a/2} \frac{Et^3}{12(1-\nu^2)}\left(\frac{\partial^2 w(x,y)}{\partial y^2} + \nu\,\frac{\partial^2 w(x,y)}{dx^2}\right) dx \quad \ldots \quad (17)$$

and the moment due to the middle-surface forces is given by

$$M_m = -\int_{-a/2}^{+a/2} E\varepsilon t w\, dx\,. \quad \ldots \quad (18)$$

The total moment acting on the cross-section of the wing is the sum of these two and it is shown in Appendix V that this may be expressed non-dimensionally in the form

$$\frac{MR}{B} = \frac{\int_{-1}^{1} D^* \left\{1 - \left(\frac{d^2w^*}{d\xi^2}\right)^2\right\} d\xi}{(1 - \nu^2)\int_{-1}^{1} D^* \, d\xi} . \qquad (19)$$

When there are no middle-surface stresses and deflections are small, $MR/B = 1$ on simple engineer's bending theory, so that the expression on the right-hand side of equation (19) provides a convenient measure of the effects of middle-surface stresses.

In the large-deflection regime w^* is not independent of the spanwise curvature and the expression above for MR/B is therefore a function of the curvature $1/R$. The flexural rigidity in the large deflection regime is

$$MR + \left(\frac{1}{R}\right)\frac{d(MR)}{d\,(1/R)} ,$$

so that the rigidity may be determined from equation (19) if w^* is known. Unfortunately it is not generally possible to obtain solutions of equation (7) in terms of known functions. An exception is the case of a solid wing, or strip, of constant thickness with a parabolic chordwise variation of strain. This case is treated in Appendix IV and the results are shown in Figs. 3 and 4. From these results it is possible to estimate the probable range of validity of small-deflection theory.

3. *Small-Deflection Theory.*—The initial distortion and stiffness of a thin solid wing of arbitrary section with an arbitrary chordwise variation of middle-surface strains will now be found. If the longitudinal curvature of the wing is small, μ tends to zero and equation (7) becomes

$$\frac{d^2}{d\xi^2}\left\{D^*\left(\frac{d^2w^*}{d\xi^2} + \nu\right)\right\} = 3\Sigma(1 - \nu^2)t^*\varepsilon^* . \qquad (20)$$

This may be integrated once to give

$$\frac{d}{d\xi}\left\{D^*\left(\frac{d^2w^*}{d\xi^2} + \nu\right)\right\} = 3\Sigma(1 - \nu^2)\int_{1}^{\xi} t^*\varepsilon^* \, d\xi , \qquad (21)$$

where the limit of integration, coupled with equation (12), has been chosen to satisfy the boundary conditions (9). Further integration gives

$$D^*\left(\frac{d^2w^*}{d\xi^2} + \nu\right) = 3\Sigma(1 - \nu^2)\int_{1}^{\xi}\int_{1}^{\xi} t^*\varepsilon^* \, d\xi \, d\xi , \qquad (22)$$

where the limit of integration, coupled with equations (12) and (13), has been chosen to satisfy the boundary conditions (8).

The initial flexural rigidity may now be obtained from equations (19) and (22) :

$$\frac{S_M}{B} = 1 + \frac{6\nu\Sigma\int_{-1}^{1}\int_{1}^{\xi}\int_{1}^{\xi} t^*\varepsilon^* \, d\xi \, d\xi \, d\xi}{\int_{-1}^{1} D^* \, d\xi} - \frac{9\Sigma^2(1 - \nu^2)\int_{-1}^{1}\left\{\frac{1}{D^*}\left(\int_{1}^{\xi}\int_{1}^{\xi} t^*\varepsilon^* \, d\xi \, d\xi\right)^2\right\} d\xi}{\int_{-1}^{1} D^* \, d\xi} . \qquad (23)$$

The distortion of the cross-section of the strip may be obtained by integrating equation (22) to give

$$w^* = A' + B'\xi - \tfrac{1}{2}\nu\xi^2 + 3\Sigma(1 - \nu^2)\int_{0}^{\xi}\int_{0}^{\xi}\left(\frac{1}{D^*}\int_{1}^{\xi}\int_{1}^{\xi} t^*\varepsilon^* \, d\xi \, d\xi\right) d\xi \, d\xi , \qquad (24)$$

where the constants A' and B' may be determined from equations (14) and (15). A convenient measure of this distortion is afforded by the camber. If we introduce the non-dimensional camber parameter Γ defined by

$$\Gamma = \frac{4R}{a^2}\{2(w)_{x=0} - (w)_{x=a/2} - (w)_{x=-a/2}\} \quad \ldots \quad (25)$$

we find, from equations (6) and (24), that

$$\left.\begin{aligned} \Gamma &= \nu - 3\Sigma(1-\nu^2)\left(\int_0^1 \psi\, d\xi + \int_0^{-1} \psi\, d\xi\right) \\ \text{where} \quad \psi &= \int_0^{\xi}\left(\frac{1}{D^*}\int_1^{\xi}\int_1^{\xi} t^*\varepsilon^*\, d\xi\, d\xi\right) d\xi \end{aligned}\right\} \quad \ldots \quad (26)$$

3.1. *Torsional Rigidity.*—For purposes of comparison the initial torsional rigidity[3,4,5] is given below :

$$\frac{S_T}{C} = 1 + \frac{3\Sigma(1+\nu)\int_{-1}^{1} \xi^2 t^*\varepsilon^*\, d\xi}{2\int_{-1}^{1} D^*\, d\xi} . \quad \ldots \quad (27)$$

Note that the final term on the right-hand side of this equation is $(1+\nu)/2\nu$ times the second term on the right-hand side of equation (23), a result that follows from the identity

$$\int_{-1}^{1}\int_1^{\xi}\int_1^{\xi} t^*\varepsilon^*\, d\xi\, d\xi\, d\xi \equiv \tfrac{1}{2}\int_{-1}^{1} \xi^2 t^*\varepsilon^*\, d\xi .$$

4. *Some Particular Cases.*—The initial flexural rigidity and distortion may always be found from equations (23) and (24) or (26) by graphical or numerical integration for any chordwise variation of t^* and ε^*. A number of important cases, however, lend themselves to exact integration, and some of these are considered below. For purposes of comparison the initial torsional rigidity is also given. Attention is generally confined to distributions of t^* and ε^* which are symmetrical about the mid-chord ($\xi = 0$). For such symmetrical distributions the limits of integration in equations (23) and (27) may be altered so that the symbols $\int_{-1}^{1}$ are replaced by $2\int_{0}^{1}$. In the first example the method of derivation is briefly outlined ; elsewhere only the results are given. Throughout, E is assumed to be constant. The results are plotted in Figs. 5 and 6.

(i) *Wing with Diamond Section and Linear Variation of ε^* from Edges to Mid-chord.*

For such a wing

$$t^* = 1 - |\xi|$$

and

$$\varepsilon^* = A_1 - |\xi| ,$$

where the constant A_1 is found from equation (12) to be $\frac{1}{3}$.

Substituting these values of t^* and ε^* in equations (23), (26) and (27) gives

$$\frac{S_M}{B} = 1 - \frac{4\nu\Sigma}{15} - \frac{7\Sigma^2(1-\nu^2)}{360}$$

$$\Gamma = \nu + \frac{\Sigma(1-\nu^2)}{6}$$

and

$$\frac{S_T}{C} = 1 - \frac{2\Sigma(1+\nu)}{15} .$$

(ii) *Wing with Diamond Section and Parabolic Variation of* ε^*.

For such a wing

$$t^* = 1 - |\xi|$$

and

$$\varepsilon^* = \frac{1}{6} - \xi^2 ,$$

so that

$$\frac{S_M}{B} = 1 - \frac{7\nu\Sigma}{30} - \frac{797\Sigma^2(1-\nu^2)}{50400}$$

$$\Gamma = \nu + \frac{19\Sigma(1-\nu^2)}{120}$$

and

$$\frac{S_T}{C} = 1 - \frac{7\Sigma(1+\nu)}{60} .$$

(iii) *Wing with Lenticular parabolic Section and Parabolic Variation of* ε^*.

For such a wing

$$t^* = 1 - \xi^2$$

and

$$\varepsilon^* = \frac{1}{5} - \xi^2 ,$$

so that

$$\frac{S_M}{B} = 1 - \frac{\nu\Sigma}{5} - \frac{\Sigma^2(1-\nu^2)}{100}$$

$$\equiv \left\{1 - \frac{\Sigma(1+\nu)}{10}\right\}\left\{1 + \frac{\Sigma(1-\nu)}{10}\right\} ,$$

$$\Gamma = \nu + \frac{\Sigma(1-\nu^2)}{10}$$

$$= -\frac{d^2w^*}{d\xi^2}$$

and

$$\frac{S_T}{C} = 1 - \frac{\Sigma(1+\nu)}{10} .$$

It will be seen that for this particular case the following simple relationship connects the flexural and torsional rigidities :

$$\frac{S_M}{B} = \frac{S_T}{C}\left\{\frac{2}{1+\nu} - \left(\frac{1-\nu}{1+\nu}\right)\left(\frac{S_T}{C}\right)\right\} . \qquad \text{.. .. ..} \qquad (28)$$

Equation (28) is valid whenever the variations with ξ of t^* and ε^* are such that the chordwise curvature, $(1/R)\ (d^2\omega^*/d\xi^2)$, is independent of ξ.

(iv) *Wing with Lenticular Parabolic Section and Quartic Variation of* ε^*.

For such a strip

$$t^* = 1 - \xi^2$$

and

$$\varepsilon^* = \frac{3}{35} - \xi^4 ,$$

so that

$$\frac{S_M}{B} = 1 - \frac{2\nu\Sigma}{15} - \frac{727\Sigma^2(1 - \nu^2)}{161700}$$

$$\Gamma = \nu + \frac{39\Sigma(1 - \nu^2)}{560}$$

and

$$\frac{S_T}{C} = 1 - \frac{\Sigma(1 + \nu)}{15} .$$

(v) *Strip of Constant Thickness with Cubic Variation of* ε^*.

This is not a practical case, but it is the simplest example of a strip with an unsymmetrical distribution of middle-surface strains.

For such a strip

$$t^* = 1$$

and

$$\bar{\varepsilon} = \Sigma'\varepsilon^* \left(\frac{t}{a}\right)^2 , \text{ say,}$$

where $\varepsilon^* = (3\xi/5) - \xi^3$ (fresh definitions of Σ' and ε^* are given here because those of equation (6) break down for this particular case) ;

whence

$$\frac{S_M}{B} = 1 - \frac{8(\Sigma')^2(1 - \nu^2)}{9625}$$

and

$$\frac{S_T}{C} = 1 .$$

Thus, due to the presence of middle-surface forces, there is a reduction in the flexural rigidity but no reduction in the torsional rigidity.

4.1. *Discussion of Results.*—In the examples the flexural rigidity vanishes (*i.e.*, flexural buckling occurs) slightly before the torsional rigidity vanishes. This result is generally true for a thin solid wing.

In the examples with a linear or parabolic stress variation the rigidities S_M and S_T become zero for values of Σ that lie in the range $5 \cdot 5 < \Sigma < 7 \cdot 5$. For the example with a quartic stress variation the rigidities become zero at an appreciably greater value of Σ (about 11). This trend reflects the fact that the middle-surface stresses tend to be more localised in the region of the leading and trailing edges, and their effect on the wing as a whole is less marked ; if the middle-surface stresses are sufficiently localised in the region of the leading and trailing edges a spanwise wavy form of instability may occur there.

As for the order of magnitude of Σ due to aerodynamic heating, it is worth noting that for Duralumin

$$\alpha \simeq 2 \cdot 3 \times 10^{-5}$$

so that if

$$T_1 - T_0 = 200° \text{ C, say,}$$

and

$$\frac{t_0}{a} = 0 \cdot 03 \text{ , say,}$$

it follows that

$$\Sigma = \alpha(T_1 - T_0) \left(\frac{a}{t_0}\right)^2$$

$$\simeq 5 \cdot 0 \text{ .}$$

5. *Conclusions.*—An exact small-deflection analysis has been presented for determining the flexural rigidity of a thin wing of arbitrary section and infinite aspect ratio with an arbitrary chordwise distribution of spanwise middle-surface stresses. Approximate bounds for the validity of this small-deflection analysis have been obtained from an exact large-deflection analysis of the flexure of a strip of rectangular section with a parabolic chordwise distribution of middle-surface stresses.

It is shown that the flexural rigidity varies with the magnitude of the middle-surface stresses (Σ) as the product of two linear terms :

$$\left(1 - \frac{\Sigma}{\Sigma_1}\right)\left(1 - \frac{\Sigma}{\Sigma_2}\right)$$

where Σ_1 and Σ_2 are of opposite sign.

The loss of flexural rigidity is comparable to the corresponding loss of torsional rigidity.

If Σ lies outside the range of Σ_1 and Σ_2, the wing buckles and assumes a spanwise curvature without the application of a bending moment.

The influence of end effects in a wing of finite aspect ratio is considered in Appendix II.

LIST OF SYMBOLS

	Ox, Oy		Cartesian axes, Oy measured spanwise, Ox measured chordwise from the mid-chord of the wing
	R		Spanwise radius of curvature of wing
	$w(x,y)$		Displacement towards the centre of spanwise curvature
	w, $w(x)$		Chordwise variation of distortion defined in equation (1)
Structural properties	E		Young's modulus, which may be a function of T and therefore of x
	E_0		Value of E at mid-chord ($x = 0$)
	ν		Poisson's ratio, assumed constant
	a		Wing chord
	t		Wing thickness (a function of x)
	D	$=$	$Et^3/\{12(1 - \nu^2)\}$
	t_0, D_0		Values of t, D at mid-chord ($x = 0$)
	S_M		Initial flexural rigidity of strip
	S_T		Initial torsional rigidity of strip
	B		Value of S_M in the absence of middle-surface stresses
		$=$	$\dfrac{1}{12}\displaystyle\int_{-a/2}^{+a/2} Et^3\,dx$
	C		Value of S_T in the absence of middle-surface stresses
		$=$	$\dfrac{2B}{1 + \nu}$
Loads and strains	ε		Spanwise middle-surface strain, measured from a stress-free datum, so that
	$E\varepsilon$		spanwise middle-surface stress (a function of x)
	$\bar{\varepsilon}$		Value of ε when the wing is flat ($R = \infty$)
	M		Total moment acting on cross-section of wing
	M_m		Part of M due to middle-surface stresses
	M_f		Part of M due to flexure about middle surface
	V_m		Strain energy per unit length due to middle-surface stresses
	V_f		Strain energy per unit length due to flexure
Non-dimensional parameters	ξ	$=$	$2x/a$
	η	$=$	$2y/a$
	t^*	$=$	Et/E_0t_0
	D^*	$=$	D/D_0
	μ	$=$	$\left\{\dfrac{3a^4(1 - \nu^2)}{16R^2t_0^2}\right\}^{1/4}$
	$w^*(\xi, \eta)$	$=$	$\left(\dfrac{4R}{a^2}\right) w(x,y)$
	w^*	$=$	$\left(\dfrac{4R}{a^2}\right) w$

LIST OF SYMBOLS—*continued*

Non-dimensional parameters:

Σ	$=$	$\left(\dfrac{a}{t_0}\right)^2 \left[(\bar{\varepsilon})_{x=0} - \tfrac{1}{2}\{(\bar{\varepsilon})_{x=a/2} + (\bar{\varepsilon})_{x=-a/2}\}\right]$
ε^*	$=$	$\bar{\varepsilon}\Big/\left[(\bar{\varepsilon})_{x=0} - \tfrac{1}{2}\{(\bar{\varepsilon})_{x=a/2} + (\bar{\varepsilon})_{x=-a/2}\}\right]$
Γ	$=$	$\dfrac{4R}{a^2}\{2(w)_{x=0} - (w)_{x=a/2} - (w)_{x=-a/2}\}$
ψ		Introduced in equation (26)
Σ'		Introduced in Section 4

α	Coefficient of thermal expansion
$T(x)$	Temperature
T_0, T_1	Values of T at mid-chord and leading or trailing edge
A_1, A_2, A', B'	Constants

Additional symbols are introduced in the Appendices.

REFERENCES

No.	Author	Title, etc.
1	H. L. Dryden and J. E. Duberg ..	Aero-elastic effects of aerodynamic heating. Paper presented to 5th General Assembly A.G.A.R.D. June, 1955.
2	L. F. Vosteen and K. E. Fuller ..	Behaviour of a cantilever plate under rapid-heating conditions. N.A.C.A. Research Memo. L.55E20c. July, 1955.
3	R. L. Bisplinghoff	Some structural and aero-elastic considerations of high-speed flight. *J.Ae.Sci.* April, 1956.
4	N. J. Hoff	Approximate analysis of the reduction in torsional rigidity and torsional buckling of solid wings under thermal stresses. *J.Ae.Sci.* June, 1956.
5	B. Budiansky and J. Mayers ..	Influence of aerodynamic heating on the effective torsional stiffness of thin wings. *J.Ae.Sci.* December, 1956.
6	J. H. Argyris	The aircraft under stress and strain. Inaugural lecture at Imperial College. London. May, 1956.
7	L. G. Brazier	*Proc. Roy. Soc.* Series A. Vol. 116, p. 104. 1927.
8	S. Timoshenko	*Theory of Plates and Shells.* McGraw-Hill. 1940.
9	H. and B. S. Jeffreys	*Methods of Mathematical Physics.* 2nd edition. Cambridge. 1950.
10	J. Kaye	The transient temperature distribution in a wing flying at supersonic speeds. *J.Ae.Sci.* December, 1950.
11	S. Timoshenko	*Theory of Elastic Stability.* 1st edition. McGraw-Hill. 1936.

APPENDIX I

Temperatures due to Aerodynamic Heating

1. A detailed method for determining the temperature distribution in a wing is given in Ref. 10. A simpler approximate method, similar to that of Ref. 5, is available if the following simplifications are made :

(*a*) The temperature does not vary across the wing thickness

(*b*) There is no heat flow in the plane of the wing

(*c*) The variation of the heat-transfer coefficient is the same for the top and bottom surface.

With these simplifications we may write for each element of the wing

$$\frac{dq}{d\tau} = 2h(T_{aw} - T) \quad \ldots \quad (29)$$

$$q = \rho \varkappa t T , \quad \ldots \quad (30)$$

where the following additional symbols have been introduced :

τ = time

h = heat-transfer coefficient

T_{aw} = adiabatic wall temperature

q = heat stored per unit area of wing

ρ = density of wing material

$\varkappa$ = specific heat of wing material.

If at time $\tau = 0$ the temperature of the wing is T' and T_{aw} is constant for $\tau > 0$, corresponding to a sudden change of velocity, the solution of equations (29) and (30) is given by

$$T - T' = (T_{aw} - T')\left\{1 - \exp\left(\frac{-2\tau'}{t^*}\right)\right\}, \quad \ldots \quad (31)$$

where

$$\tau' = \frac{h\tau}{\rho \varkappa t_0} .$$

Some typical chordwise temperature distributions at various values of τ' are shown in Fig. 7 for solid wings of diamond and lenticular parabolic section, assuming h constant. These temperature distributions may be converted to stress distributions by using equation (12).

APPENDIX II

End Effects in a wing of Finite Aspect Ratio

1. *Influence of End Effects on the Middle-Surface Stresses.*—The analysis given in the main body of the report is strictly applicable to a wing of infinite aspect ratio. In a wing of finite aspect ratio the spanwise middle-surface stresses necessarily fall to zero at the wing tips. In the neighbourhood of the wing tips there will therefore be a region where the stress pattern is changing. The magnitude of this 'end effect' may be readily estimated by assuming that

(*a*) the chordwise variation of spanwise stresses remains unaltered

(*b*) the magnitude of the 'end effect' stresses decays exponentially from the tip

(*c*) chordwise strains may be ignored.

With these assumptions the problem reduces to the determination of the exponent of the stress decay, which may be found from energy considerations. We shall apply a longitudinal displacement $v_0 = a\bar{\varepsilon}$ to one end of a semi-infinite strip and determine the strain energy of the strip. From assumption (*b*) we have

$$v = a\bar{\varepsilon} \exp\left(-\frac{y}{a\beta}\right), \qquad \qquad (32)$$

where β is a decay length parameter. On differentiating to obtain the stresses we find

$$\begin{aligned} \sigma_y &= E\frac{\partial v}{\partial y} \\ &= -\frac{E\bar{\varepsilon}}{\beta}\exp\left(-\frac{y}{a\beta}\right) \end{aligned}$$

and

$$\begin{aligned} \tau_{xy} &= \frac{E}{2(1+\nu)}\frac{\partial v}{\partial x} \\ &= \frac{Ea}{2(1+\nu)}\frac{d\bar{\varepsilon}}{dx}\exp\left(-\frac{y}{a\beta}\right). \end{aligned}$$

The strain energy of the strip is given by

$$\begin{aligned} V &= \int_0^\infty \int_{-a/2}^{a/2} \frac{t}{2E}\left\{\sigma_y^2 + 2(1+\nu)\tau_{xy}^2\right\} dx\, dy \\ &= \int_0^\infty \int_{-a/2}^{a/2} \frac{Et}{2}\left\{\frac{(\bar{\varepsilon})^2}{\beta^2} + \frac{a^2(d\bar{\varepsilon}/dx)^2}{2(1+\nu)}\right\}\exp\left(-\frac{2y}{a\beta}\right) dx\, dy\,. \end{aligned}$$

In terms of non-dimensional functions it is found, after integrating with respect to y, that

$$V \propto \frac{1}{\beta}\int_{-1}^{1} t^*(\varepsilon^*)^2\, d\xi + \frac{2\beta}{1+\nu}\int_{-1}^{1} t^*\left(\frac{d\varepsilon^*}{d\xi}\right)^2 d\xi \qquad \qquad (33)$$

and β is found from the condition that this is a minimum with respect to β, whence

$$\beta^2 = \frac{(1+\nu)\int_{-1}^{1} t^*(\varepsilon^*)^2\, d\xi}{2\int_{-1}^{1} t^*\left(\dfrac{d\varepsilon^*}{d\xi}\right)^2 d\xi}\,. \qquad \qquad (34)$$

Values of β for examples (i) to (iv) of Section 4 are given below assuming $\nu = 0 \cdot 3$:

Example Number	(i)	(ii)	(iii)	(iv)
β	0·190	0·195	0·193	0·140

The magnitude of the spanwise middle-surface stresses varies as

$$\left\{1 - \exp\left(-\frac{y}{a\beta}\right)\right\}$$

in the region of the wing tip, y being zero at the tip. For a wing of rectangular plan-form measuring $2l \times a$, there are two end effects and the magnitude of the spanwise middle-surface stresses varies as

$$\left(1 - \frac{\cosh(y/a\beta)}{\cosh(l/a\beta)}\right),$$

where y is zero at the centre-line.

The end effects are confined roughly to a distance of βa from a tip and it follows from the Table above that the tip end effect is only important for wings of aspect ratio less than about 2, though it may be readily determined from the present analysis.

There is a further 'end effect' in a wing as shown in Fig. 8, in which the central region is at a uniform temperature. This central region acts in the nature of a buffer between the outer regions, and if sufficiently long it can reduce the middle-surface stresses at the junction sections by 50 per cent. It can be readily verified that the magnitude of the spanwise middle surface stresses in the outer regions is now given by

$$\frac{\Sigma(y)}{\Sigma} = 1 - \left[\frac{\sinh(l_0/a\beta)\sinh\{(l_1 - y)/a\beta\} + \cosh\{(l_0 + y)/a\beta\}}{\cosh\{(l_0 + l_1)/a\beta\}}\right], \quad \ldots \quad (35)$$

where y is measured from the junction section.

In the central region

$$\frac{\Sigma(y)}{\Sigma} = \frac{\{\cosh(l_1/a\beta) - 1\}\cosh(y/a\beta)}{\cosh\{(l_0 + l_1)/a\beta\}}, \quad \ldots \quad \ldots \quad \ldots \quad \ldots \quad \ldots \quad (36)$$

where y is measured from the centre section.

Some examples of equations (35) and (36) are shown in Fig. 9, assuming $\beta = 0 \cdot 19$ and $l_1 = 1 \cdot 5a$ for values of $l_0/a = 0, 0 \cdot 25, 0 \cdot 5$.

The flexural or torsional rigidity at any section may be determined from the analysis in the main body of the report, using $\Sigma(y)$ instead of Σ.

2. *End Effect due to Building-in.*—Where a wing is built-in, its cross-section is prevented from distorting and the flexural rigidity at that section will be unaffected by middle-surface stresses. In the vicinity of a built-in section there will therefore be a region of varying flexural rigidity. This end effect may be estimated in a manner similar to that used for the tip end effect. The following assumptions are made :

(*a*) The chordwise variation of the distortion is constant

(*b*) The spanwise variation of the distortion varies as

$$\left(1 + \frac{y}{a\gamma}\right)\exp\left(-\frac{y}{a\gamma}\right),$$

the linear term ensuring that $\partial w/\partial y$ vanishes at the built-in section.

The parameter γ is to be chosen so that the strain energy of the strip is a minimum. It is found that the strain energy V is proportional to

$$80\gamma \int_{-1}^{1} D^* \left(\frac{d^2w^*}{d\xi^2}\right)^2 d\xi + \frac{8}{\gamma} \int_{-1}^{1} D^* \left\{(1-\nu)\left(\frac{dw^*}{d\xi}\right)^2 - \nu w^* \frac{d^2w^*}{d\xi^2}\right\} d\xi$$

$$+ \frac{1}{\gamma^3} \int_{-1}^{1} D^*(w^*)^2 \, d\xi$$

and the condition that this is a minimum with respect to γ yields the following equation for γ

$$80\gamma^4 \int_{-1}^{1} D^* \left(\frac{d^2w^*}{d\xi^2}\right)^2 d\xi - 8\gamma^2 \int_{-1}^{1} D^* \left\{(1-\nu)\left(\frac{dw^*}{d\xi}\right)^2 - \nu w^* \frac{d^2w^*}{d\xi^2}\right\} d\xi$$

$$- 3 \int_{-1}^{1} D^*(w^*)^2 \, d\xi = 0 . \quad \ldots \quad (37)$$

The chordwise distortion w^* is given by equation (24); but some improvement in accuracy may be achieved by choosing the constant A' (or B') differently.

If we confine attention to the case when B' is zero and regard A' as unknown, we can minimise V with respect to A' and determine the following equation for A'

$$\int_{-1}^{1} D^* w^* \, d\xi = 4\nu\gamma^2 \int_{-1}^{1} D^* \frac{d^2w^*}{d\xi^2} d\xi . \quad \ldots \quad (38)$$

In view of the complexity of equations (24) and (37), an approximate value for γ may be obtained by writing

$$w^* \propto A' - \tfrac{1}{2}\xi^2 . \quad \ldots \quad (39)$$

After eliminating A' by using equation (38) and substituting in equation (37), the following equation for γ results:

$$\left.\begin{aligned} &64\gamma^4 I_0^2(5-\nu^2) - 32\gamma^2 I_0 I_2(1-\nu) + 3(I_2^2 - I_0 I_4) = 0 , \\ &\text{where} \quad I_n = \int_{-1}^{1} \xi^n D^* \, d\xi \end{aligned}\right\} \quad \ldots \quad (40)$$

Values of γ for a diamond-section wing and for a lenticular-parabolic-section wing, obtained from equation (40), are given below

Diamond section ..	$\gamma = 0 \cdot 111$
Parabolic section ..	$\gamma = 0 \cdot 133$

It should be noted that the value of $0 \cdot 133$ for γ is strictly correct (within the framework of the above assumptions) for example (iii) of the main text. This is because the true variation of w^* in example (iii) is the same as that of equation (39).

This end effect is confined roughly to a distance of $2\gamma a$ from the built-in section. The influence of this end effect is confined to the flexural rigidity; the torsional rigidity is unaffected.

The spanwise variation of the flexural rigidity is given approximately by

$$S_M(y) = (S_M)_{\Sigma(y)} + \left\{\frac{B}{1-\nu^2} - (S_M)_{\Sigma(y)}\right\}\left(1 + \frac{y}{a\gamma}\right) \exp\left(\frac{-y}{a\gamma}\right) , \quad \ldots \quad (41)$$

where y is measured from the built-in section and $(S_M)_{\Sigma(y)}$ is the value of S_M appropriate to the local value of $\Sigma(y)$.

APPENDIX III

Analysis for a Built-up Wing

1. In considering a built-up wing, it is necessary to introduce the following symbols :

t		(overall) thickness of wing
$\bar{t}$		total thickness of spanwise stress-bearing material
$\bar{t}^*$	$=$	$\dfrac{E\bar{t}}{(E\bar{t})_0}$
ν_x, ν_y		values of Poisson's ratio in x and y directions (*see* Ref. 11, p. 381)
EI_x, EI_y		flexural rigidities/unit length in the absence of middle-surface stresses (*see* Ref. 11, p. 381)
D_x^*	$=$	$\dfrac{EI_x}{(EI_x)_0}$
D_y^*	$=$	$\dfrac{EI_y}{(EI_y)_0}$
λ	$=$	$\dfrac{\bar{t}_0 t_0^2}{12 I_{x,0}}$, which tends to unity as the solidity of the wing increases.

The differential equation governing the chordwise distortion of the wing (*cf.* equation (5)) is now

$$\frac{d^2}{dx^2}\left\{\frac{EI_x}{(1-\nu_x\nu_y)}\left(\frac{d^2w}{dx^2}+\frac{\nu_y}{R}\right)\right\}-\frac{E\bar{t}}{R}\left(\bar{\varepsilon}-\frac{w}{R}\right)=0\,. \quad \ldots \quad (42)$$

Confining attention to the small deflection regime, in which w/R may be neglected in comparison with $\bar{\varepsilon}$, equation (42) may be written non-dimensionally in the form

$$\frac{d^2}{d\xi^2}\left\{D_x^*\left(\frac{d^2w^*}{d\xi^2}+\nu_y\right)\right\}=3\lambda\Sigma(1-\nu_x\nu_y)\bar{t}^*\varepsilon^*\,. \quad \ldots \quad (43)$$

This equation may be integrated in a similar manner to that described in Section 3 to give

$$D_x^*\left(\frac{d^2w^*}{d\xi^2}+\nu_y\right)=3\lambda\Sigma(1-\nu_x\nu_y)\int_1^\xi\int_1^\xi \bar{t}^*\varepsilon^*\,d\xi\,d\xi \ldots \quad (44)$$

The moment due to flexure about the middle surface of the wing is given by

$$M_f=\int_{-a/2}^{a/2}\frac{EI_y}{(1-\nu_x\nu_y)}\left\{\frac{\partial^2 w(x,y)}{\partial y^2}+\nu_x\frac{\partial^2 w(x,y)}{\partial x^2}\right\}dx \quad \ldots \quad (45)$$

and the moment due to the middle surface forces is given by

$$\begin{aligned} M_m &= -\int_{-a/2}^{a/2} E\varepsilon\bar{t}w\,dx \\ &= -\int_{-a/2}^{a/2} w\,\frac{d^2}{dx^2}\left\{\frac{EI_x}{(1-\nu_x\nu_y)}\left(R\,\frac{d^2w}{dx^2}+\nu_y\right)\right\}dx \quad \ldots \quad (46)\end{aligned}$$

by virtue of equation (42).

The total moment acting on the cross-section of the wing is the sum of these two and may be expressed non-dimensionally, after integrating by parts as in Appendix V, in the form

$$\frac{2MR(1-\nu_x\nu_y)}{a(EI_y)_0} = \int_{-1}^{1} D_y^* \left(1+\nu_x \frac{d^2w^*}{d\xi^2}\right) d\xi$$
$$- \left(\frac{I_x}{I_y}\right)_0 \int_{-1}^{1} D_x^* \frac{d^2w^*}{d\xi^2}\left(\frac{d^2w^*}{d\xi^2}+\nu_y\right) d\xi \, . \quad \ldots \quad \ldots \quad \ldots \quad (47)$$

The initial flexural rigidity of the wing S_M is equal to the initial value of MR and if we write

$$B = \tfrac{1}{2}a(EI_y)_0 \int_{-1}^{1} D_y^* \, d\xi \, ,$$

we find from equations (44) and (47) that

$$\frac{S_M}{B} = 1 + \frac{3\lambda\Sigma \int_{-1}^{1}\left[\left\{\nu_x\left(\frac{D_y^*}{D_x^*}\right)+\nu_y\left(\frac{I_x}{I_y}\right)_0\right\}\int_1^{\xi}\int_1^{\xi}\bar{t}^*\varepsilon^*\,d\xi\,d\xi\right]d\xi}{\int_{-1}^{1} D_y^*\,d\xi}$$
$$- \frac{9\lambda^2\Sigma^2(1-\nu_x\nu_y)(I_x/I_y)_0 \int_{-1}^{1}\left\{\frac{1}{D_x^*}\left(\int_1^{\xi}\int_1^{\xi}\bar{t}^*\varepsilon^*\,d\xi\,d\xi\right)^2\right\}d\xi}{\int_{-1}^{1} D_y^*\,d\xi} \, . \quad (48)$$

Some simplification of equation (48) is possible for a wing consisting simply of a top and bottom skin (which may be relatively thick) and a stabilising filling. For such a wing

$$\left.\begin{aligned} I_x &= I_y \\ D_x^* &= D_y^* \\ \nu_x &= \nu_y = \nu \end{aligned}\right\} , \quad \ldots \quad \ldots \quad \ldots \quad \ldots \quad \ldots \quad \ldots \quad \ldots \quad \ldots \quad (49)$$

so that equation (48) becomes

$$\frac{S_M}{B} = 1 + \frac{6\nu\lambda\Sigma \int_{-1}^{1}\int_1^{\xi}\int_1^{\xi}\bar{t}^*\varepsilon^*\,d\xi\,d\xi\,d\xi}{\int_{-1}^{1} D_y^*\,d\xi}$$
$$- \frac{9\lambda^2\Sigma^2(1-\nu^2)\int_{-1}^{1}\left\{\frac{1}{D_y^*}\left(\int_1^{\xi}\int_1^{\xi}\bar{t}^*\varepsilon^*\,d\xi\,d\xi\right)^2\right\}d\xi}{\int_{-1}^{1} D_y^*\,d\xi} \, . \quad \ldots \quad \ldots \quad (50)$$

When the wing is solid, $\bar{t} = t$, so that $\lambda = 1$, and equation (50) reduces to equation (23) of the main text. For purposes of comparison with the solid wing it is convenient to consider the limiting case of a wing with a thin skin of constant thickness $(\frac{1}{2}\bar{t})$. For such a wing

$$I_x = (\tfrac{1}{2}t)^2 \times \bar{t} \, ,$$

so that

$$\lambda = \tfrac{1}{3} \, . \quad \ldots \quad \ldots \quad \ldots \quad \ldots \quad \ldots \quad \ldots \quad \ldots \quad \ldots \quad \ldots \quad (51)$$

Two examples are now given.

(*a*) *Hollow Wing of Diamond Section and Parabolic Variation of Strain.*

For such a wing

$$\bar{t}^* = 1 ,$$

if the skin thickness does not vary, so that

$$\varepsilon^* = \tfrac{1}{3} - \xi^2$$

and

$$D_y^* = (1 - |\xi|)^2$$

and from equation (50)

$$\frac{S_M}{B} = 1 - \frac{4\nu\Sigma}{15} - \frac{11\Sigma^2(1 - \nu^2)}{560} ,$$

while from Refs. 3, 4 and 5 (bearing in mind the fact that, because of the stabilising filling, the wing acts as a ' plate ' instead of a hollow tube) :

$$\frac{S_T}{C} = 1 - \frac{2\Sigma(1 + \nu)}{15} .$$

(*b*) *Hollow Wing of Lenticular Parabolic Section and Parabolic Variation of Strain.*

For such a wing

$$D_y^* = (1 - \xi^2)^2 ,$$

so that

$$\frac{S_M}{B} = \left\{1 - \frac{\Sigma(1 + \nu)}{12}\right\}\left\{1 + \frac{\Sigma(1 - \nu)}{12}\right\} ,$$

while from Refs. 3, 4 and 5

$$\frac{S_T}{C} = 1 - \frac{\Sigma(1 + \nu)}{12} .$$

2. *Discussion.*—The variations of the flexural and torsional rigidities with Σ for examples (*a*) and (*b*) above are shown in Fig. 10.

It should be noted that in the above examples the skin thickness was constant and, if the heat capacity of the stabilising filling could be ignored, there would be no chordwise temperature gradients due to aerodynamic heating unless the heat-transfer coefficient varies in the chordwise direction.

APPENDIX IV

Large-Deflection Solution for a Solid Strip of Constant Thickness

1. We consider here the behaviour of a strip of constant thickness with a parabolic chordwise variation of temperature and a constant value of E. For such a simple case the differential equation (7) may be readily formulated and solved.

We have

$$T(x) = T_0 + (T_1 - T_0)\left(\frac{2x}{a}\right)^2, \quad \ldots \quad (52)$$

so that

$$\bar{\varepsilon} = \alpha(T_1 - T_0)\left\{\frac{1}{3} - \left(\frac{2x}{a}\right)^2\right\}, \quad \ldots \quad (53)$$

by virtue of equations (12) and (13). Further,

$$t^* = D^* = 1\,, \quad \ldots \quad (54)$$

so that equation (7) reduces to

$$\left.\begin{aligned} \frac{d^4w^*}{d\xi^4} + 4\mu^4 w^* &= 3\Sigma(1 - \nu^2)\left(\frac{1}{3} - \xi^2\right) \\ \text{where} \qquad \Sigma &= \alpha(T_1 - T_0)\left(\frac{a}{t}\right)^2 \end{aligned}\right\} \quad \ldots \quad (55)$$

The solution of equation (55) subject to the boundary conditions (8) and (9) is given by

$$w^* = \frac{\Sigma(1-\nu^2)(1-3\xi^2)}{4\mu^4} + \left(\frac{3\Sigma(1-\nu^2)}{4\mu^6} - \frac{\nu}{2\mu^2}\right)\left\{\left(\frac{c\mathscr{S} - \mathscr{C}s}{\mathscr{C}\mathscr{S} + cs}\right)\cosh\mu\xi\cos\mu\xi + \left(\frac{c\mathscr{S} + \mathscr{C}s}{\mathscr{C}\mathscr{S} + cs}\right)\sinh\mu\xi\sin\mu\xi\right\}, \quad \ldots \quad (56)$$

where $\mathscr{C}$, $\mathscr{S}$, c, s stand for $\cosh\mu$, $\sinh\mu$, $\cos\mu$, $\sin\mu$ respectively.

2. *Bending-Moment–Curvature Relationship.*—The bending-moment–curvature relationship is obtained by substituting equation (56) in equation (19), whence

$$\frac{MR}{B} = \frac{1 - \nu^2\phi_1}{1 - \nu^2} - \nu\Sigma\phi_2 - \Sigma^2(1-\nu^2)\phi_3\,, \quad \ldots \quad (57)$$

where

$$\left.\begin{aligned} \phi_1 &= \frac{3(\mathscr{S}^2 + s^2)}{4\mu(\mathscr{C}\mathscr{S} + cs)} + \frac{\mathscr{C}\mathscr{S}cs}{(\mathscr{C}\mathscr{S} + cs)^2} \\ \phi_2 &= \frac{3}{\mu^4}\left\{\frac{\mathscr{S}^2 + s^2}{4\mu(\mathscr{C}\mathscr{S} + cs)} - \frac{\mathscr{C}\mathscr{S}cs}{(\mathscr{C}\mathscr{S} + cs)^2}\right\} \\ \phi_3 &= \frac{9}{4\mu^8}\left\{1 - \frac{5(\mathscr{S}^2 + s^2)}{4\mu(\mathscr{C}\mathscr{S} + cs)} + \frac{\mathscr{C}\mathscr{S}cs}{(\mathscr{C}\mathscr{S} + cs)^2}\right\} \end{aligned}\right\} \quad \ldots \quad (58)$$

The variation of MR/B against $a^2/(Rt)$, i.e., against $2{\cdot}42\mu^2$, is plotted in Fig. 3 for various values of Σ. The variation of $(Ma^2)/Bt$ with $a^2/(Rt)$ (i.e., the bending-moment–curvature relationship) is plotted in Fig. 4 for various values of Σ.

The initial flexural rigidity vanishes when $\Sigma = 5{\cdot}07$. For values of Σ greater than this critical value the strip assumes a spanwise curvature without the application of a bending moment. For example, if $\Sigma = 7$, it is seen from Figs. 3 or 4 that $a^2/(Rt) = 3{\cdot}64$ when the strip is unloaded.

APPENDIX V

Total Moment Acting on Cross-Section of Strip

1. The total moment acting on a cross-section of the strip is obtained from equations (17) and (18). In non-dimensional form these equations reduce to

$$\frac{MR}{B} = \frac{\int_{-1}^{1} \left[D^* \left(1 + \nu \frac{d^2 w^*}{d\xi^2}\right) - w^* t^* \{3\Sigma\varepsilon^*(1 - \nu^2) - 4\mu^4 w^*\} \right] d\xi}{(1 - \nu^2) \int_{-1}^{1} D^* \, d\xi} \quad \ldots \quad \ldots \quad (59)$$

The numerator of this expression simplifies considerably. From equation (7) the numerator may be written as

$$\int_{-1}^{1} D^* \left(1 + \nu \frac{d^2 w^*}{d\xi^2}\right) d\xi - \int_{-1}^{1} \left[w^* \frac{d^2}{d\xi^2} \left\{ D^* \left(\frac{d^2 w^*}{d\xi^2} + \nu \right) \right\} \right] d\xi$$

$$= \int_{-1}^{1} D^* \left(1 + \nu \frac{d^2 w^*}{d\xi^2}\right) d\xi - \left[w^* \frac{d}{d\xi} \left\{ D^* \left(\frac{d^2 w^*}{d\xi^2} + \nu \right) \right\} \right]_{-1}^{1}$$

$$+ \int_{-1}^{1} \left(\frac{dw^*}{d\xi} \right) \frac{d}{d\xi} \left\{ D^* \left(\frac{d^2 w^*}{d\xi^2} + \nu \right) \right\} d\xi$$

on integrating by parts. Further, by virtue of the boundary condition (9), the middle term above vanishes. Integration by parts again gives

$$\int_{-1}^{1} D^* \left(1 + \nu \frac{d^2 w^*}{d\xi^2}\right) d\xi + \left[D^* \frac{dw^*}{d\xi} \left(\frac{d^2 w^*}{d\xi^2} + \nu \right) \right]_{-1}^{1} - \int_{-1}^{1} D^* \left(\frac{d^2 w^*}{d\xi^2} + \nu \right) \frac{d^2 w^*}{d\xi^2} \, d\xi$$

$$= \int_{-1}^{1} D^* \left\{ 1 - \left(\frac{d^2 w^*}{d\xi^2} \right)^2 \right\} d\xi ,$$

by virtue of the boundary condition (8).

Equation (19) follows from these results.

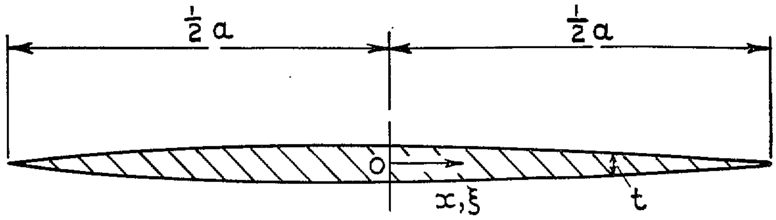

FIG. 1. Cross-section of wing.

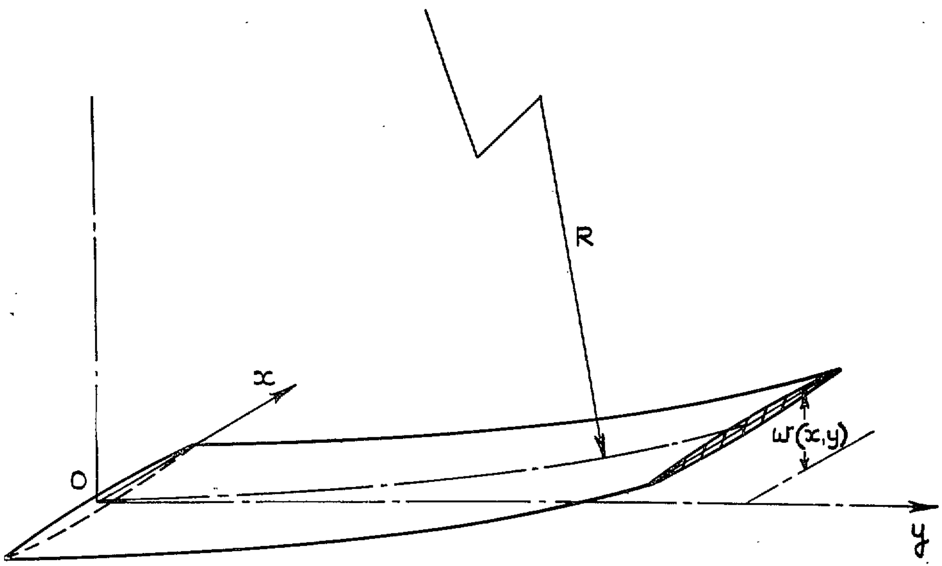

FIG. 2. The distorted wing.

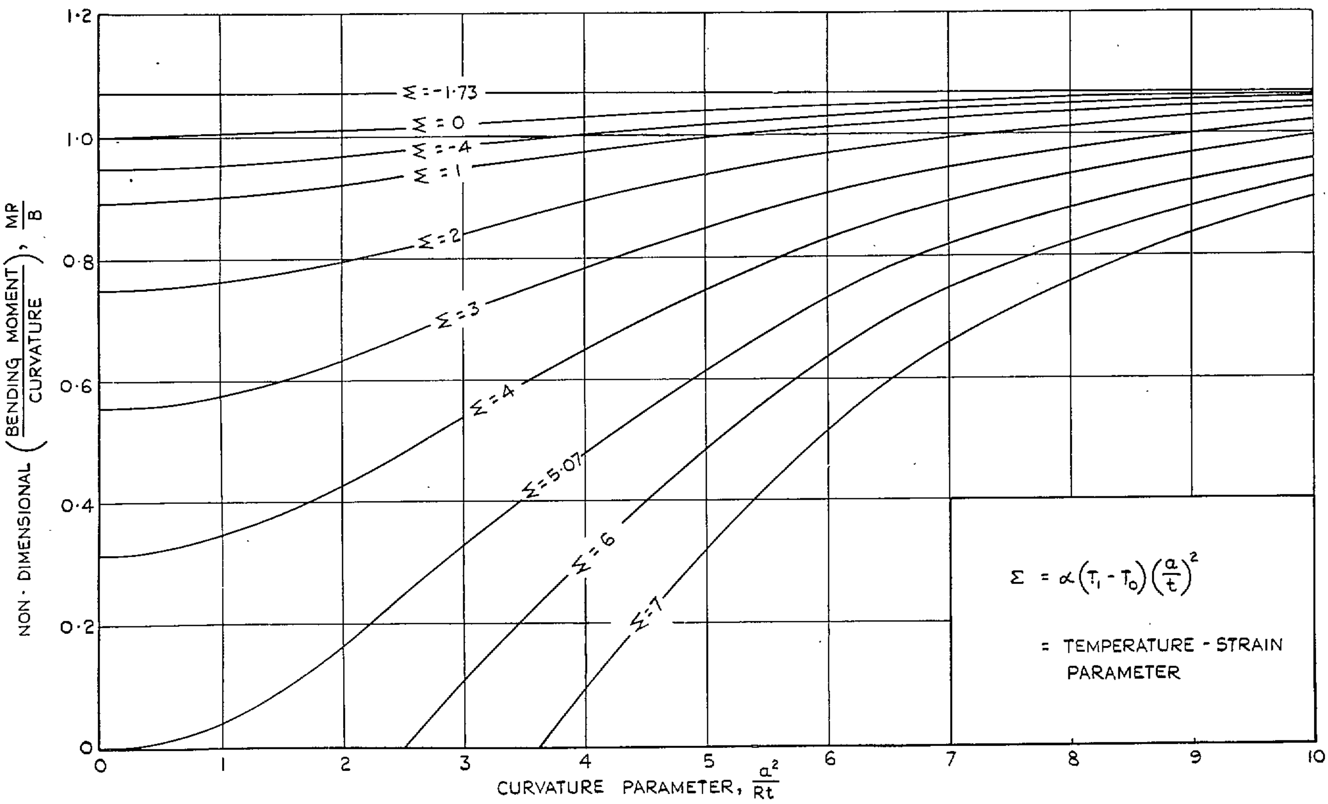

FIG. 3. Variation of MR/B with curvature for strip of constant thickness and parabolic temperature distribution.

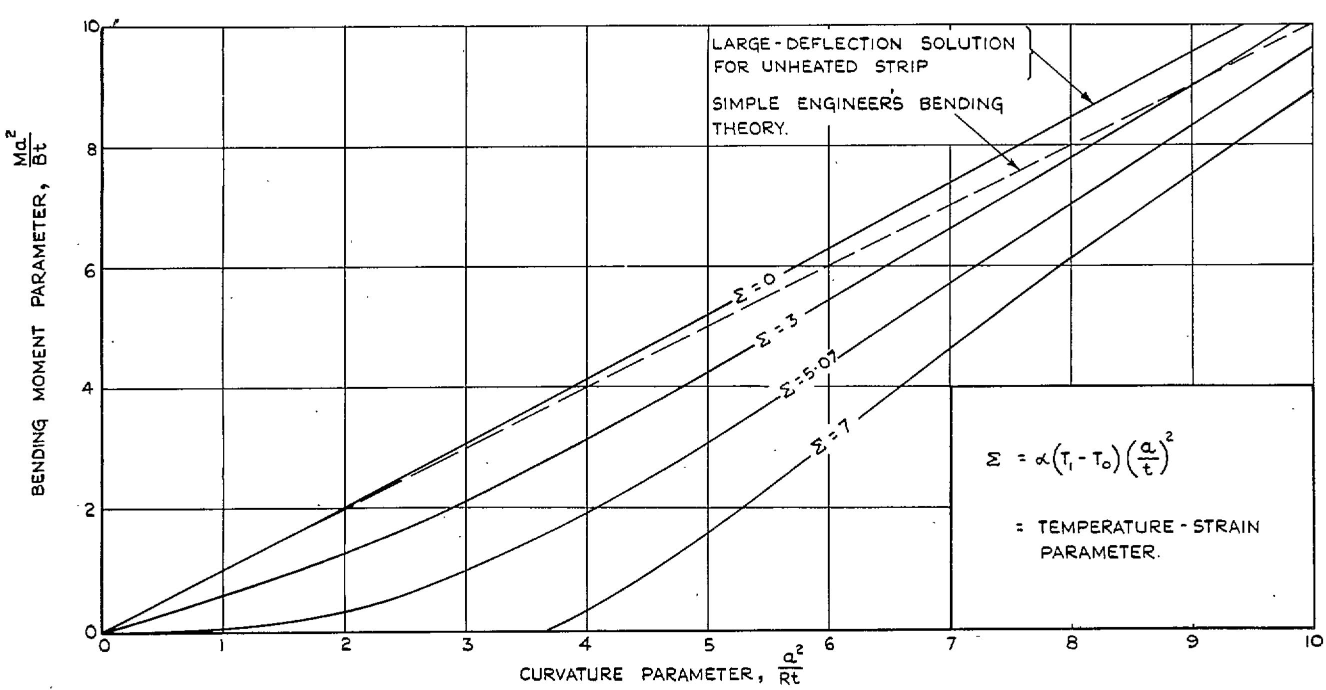

FIG. 4. Variation of bending moment with curvature for strip of constant thickness and parabolic temperature distribution.

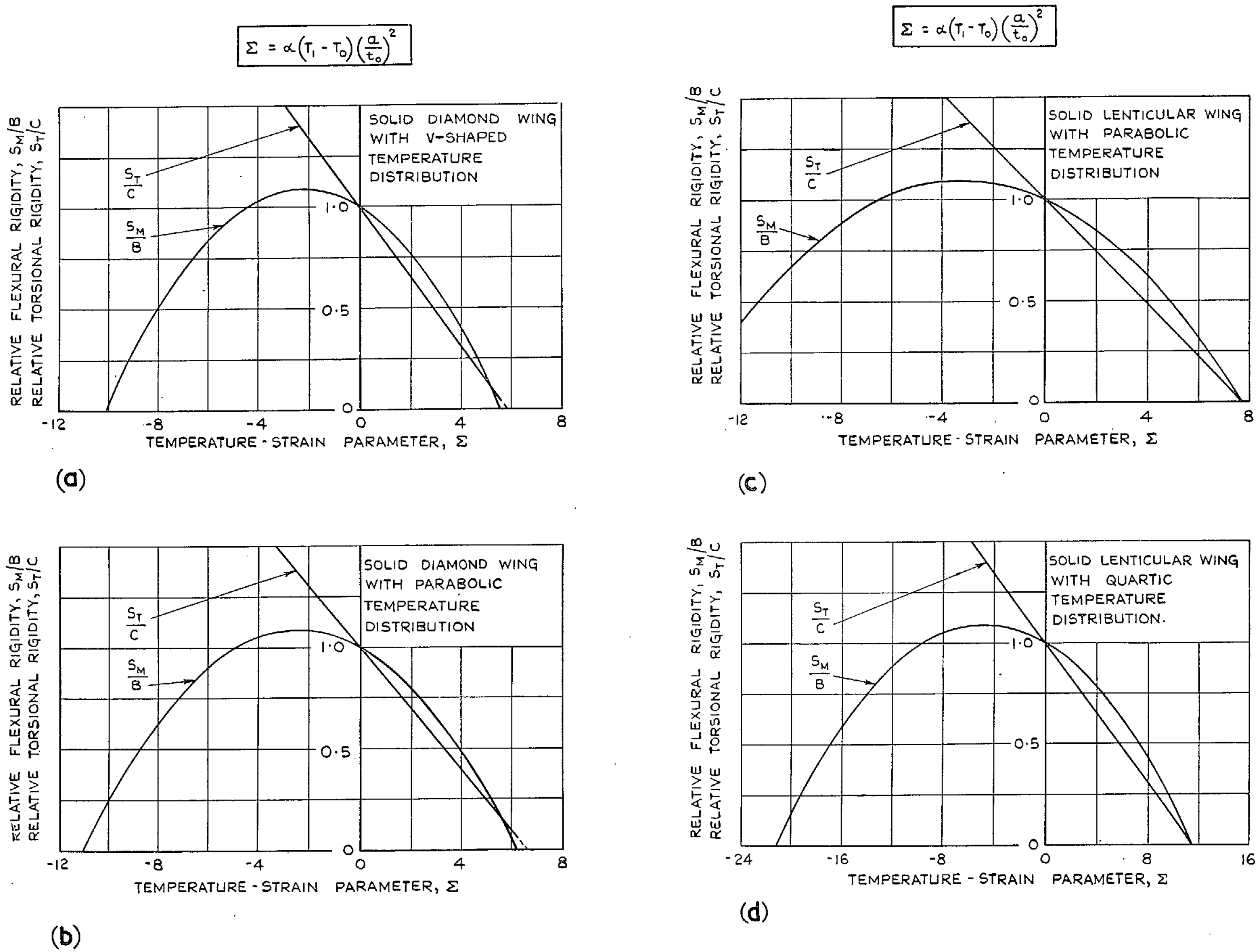

FIGS. 5a to 5d. Variation of flexural and torsional rigidities with temperature-strain parameter.

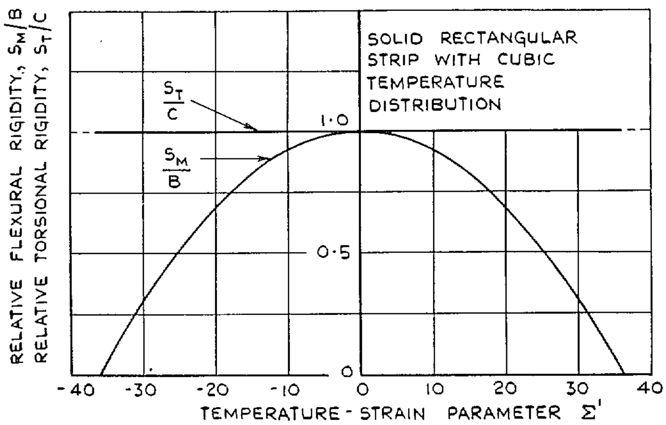

(e)

FIG. 5e. Variation of flexural and torsional rigidities with temperature-strain parameter.

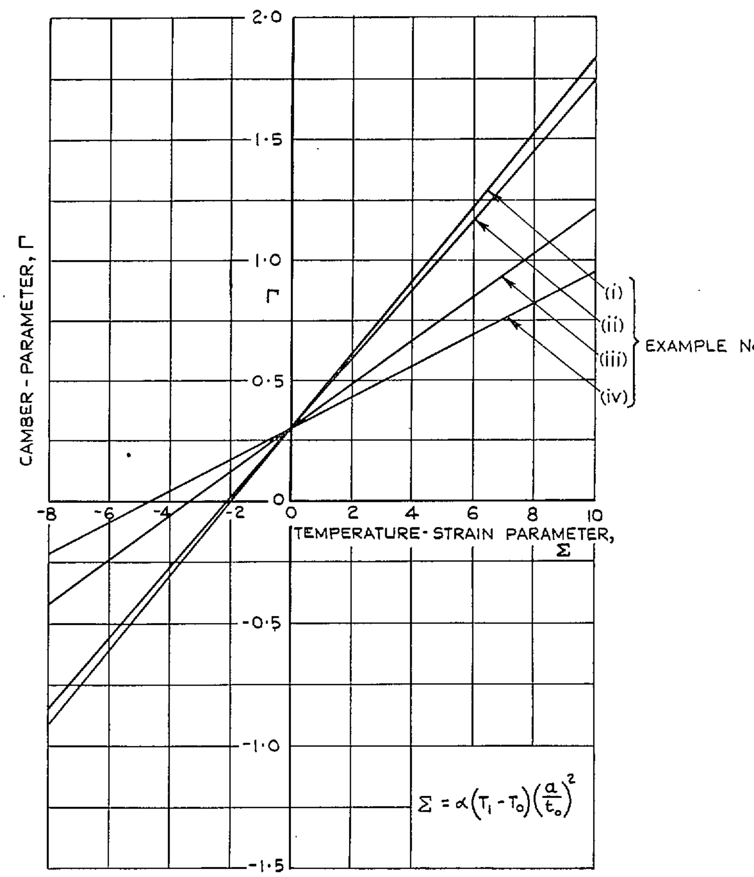

FIG. 6. Variation of camber parameter with temperature-strain parameter.

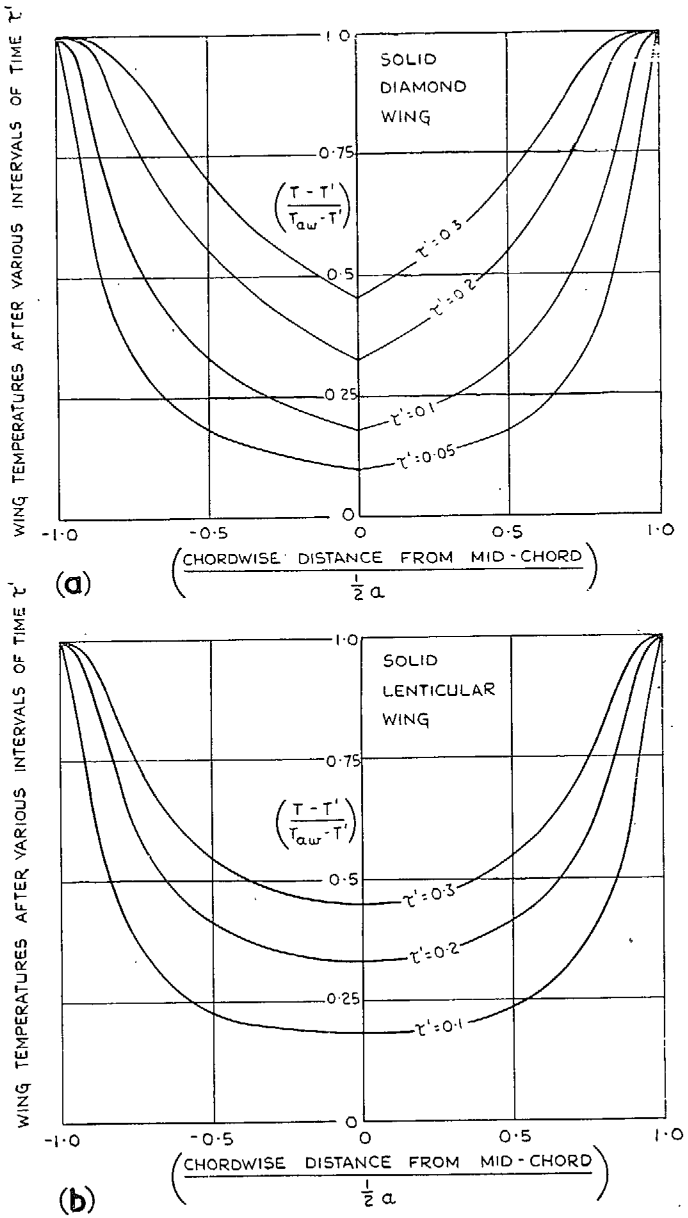

FIGS. 7a and 7b. Typical chordwise variations of temperature after sudden increase of velocity (*See* Appendix I).

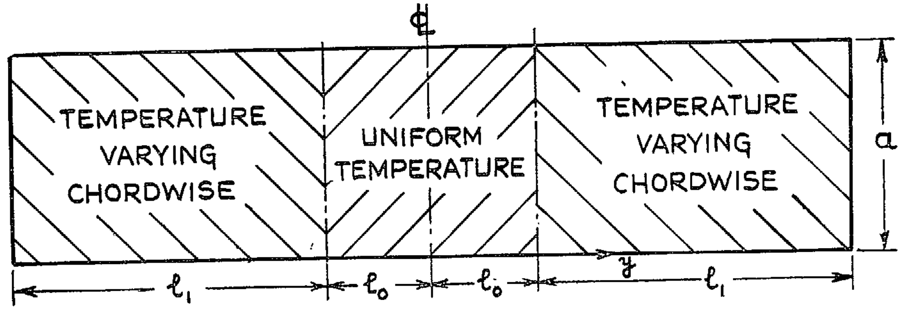

FIG. 8. Wing of finite aspect ratio.

(74984) Wt. 53/2293 K.7 9/59 Hw.

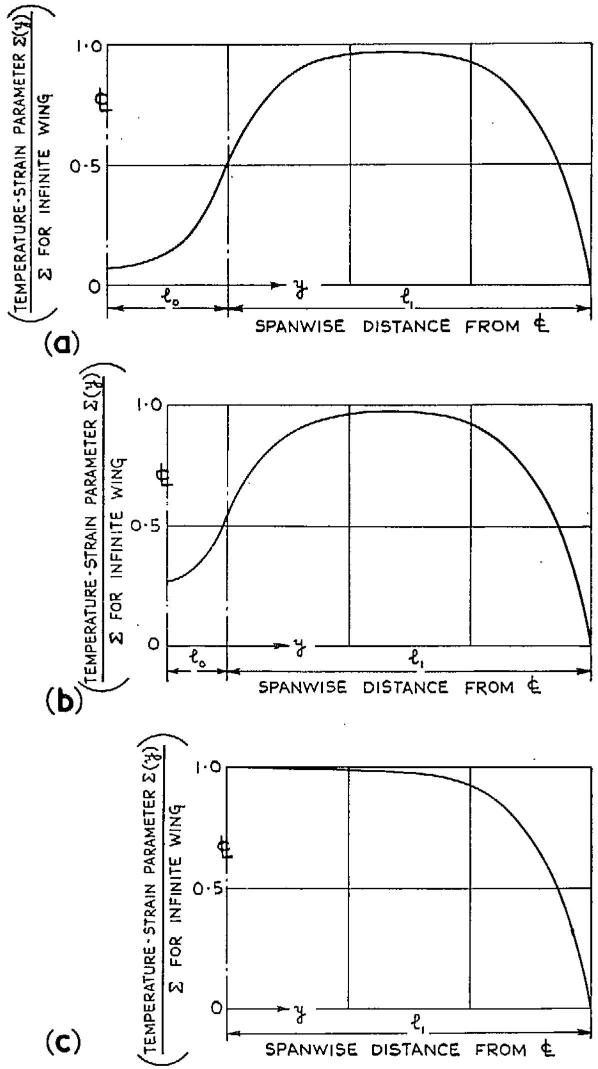

FIGS. 9a to 9c. Typical spanwise variations of middle-surface stresses.

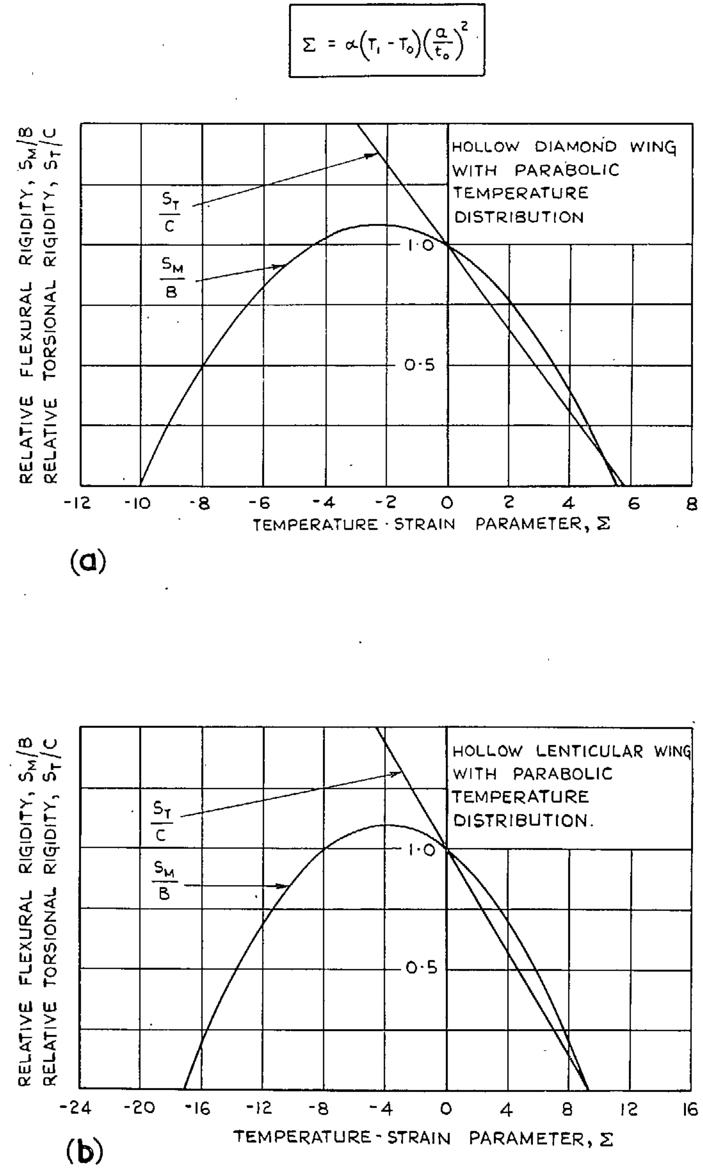

FIGS. 10a and 10b. Variation of flexural and torsional rigidities with temperature-strain parameter.

PRINTED IN GREAT BRITAIN

Publications of the Aeronautical Research Council

ANNUAL TECHNICAL REPORTS OF THE AERONAUTICAL RESEARCH COUNCIL (BOUND VOLUMES)

1939 Vol. I. Aerodynamics General, Performance, Airscrews, Engines. 50*s*. (52*s*.).
Vol. II. Stability and Control, Flutter and Vibration, Instruments, Structures, Seaplanes, etc. 63*s*. (65*s*.)

1940 Aero and Hydrodynamics, Aerofoils, Airscrews, Engines, Flutter, Icing, Stability and Control, Structures, and a miscellaneous section. 50*s*. (52*s*.)

1941 Aero and Hydrodynamics, Aerofoils, Airscrews, Engines, Flutter, Stability and Control, Structures. 63*s*. (65*s*.)

1942 Vol. I. Aero and Hydrodynamics, Aerofoils, Airscrews, Engines. 75*s*. (77*s*.)
Vol. II. Noise, Parachutes, Stability and Control, Structures, Vibration, Wind Tunnels. 47*s*. 6*d*. (49*s*. 6*d*.)

1943 Vol. I. Aerodynamics, Aerofoils, Airscrews. 80*s*. (82*s*.)
Vol. II. Engines, Flutter, Materials, Parachutes, Performance, Stability and Control, Structures. 90*s*. (92*s*. 9*d*.)

1944 Vol. I. Aero and Hydrodynamics, Aerofoils, Aircraft, Airscrews, Controls. 84*s*. (86*s*. 6*d*.)
Vol. II. Flutter and Vibration, Materials, Miscellaneous, Navigation, Parachutes, Performance, Plates and Panels, Stability, Structures, Test Equipment, Wind Tunnels. 84*s*. (86*s*. 6*d*.)

1945 Vol. I. Aero and Hydrodynamics, Aerofoils. 130*s*. (132*s*. 9*d*.)
Vol. II. Aircraft, Airscrews, Controls. 130*s*. (132*s*. 9*d*.)
Vol. III. Flutter and Vibration, Instruments, Miscellaneous, Parachutes, Plates and Panels, Propulsion. 130*s*. (132*s*. 6*d*.)
Vol. IV. Stability, Structures, Wind Tunnels, Wind Tunnel Technique. 130*s*. (132*s*. 6*d*.)

Annual Reports of the Aeronautical Research Council—

1937 2*s*. (2*s*. 2*d*.) 1938 1*s*. 6*d*. (1*s*. 8*d*.) 1939–48 3*s*. (3*s*. 5*d*.)

Index to all Reports and Memoranda published in the Annual Technical Reports, and separately—

April, 1950 - - - - R. & M. 2600 2*s*. 6*d*. (2*s*. 10*d*.)

Author Index to all Reports and Memoranda of the Aeronautical Research Council—

1909—January, 1954 R. & M. No. 2570 15*s*. (15*s*. 8*d*.)

Indexes to the Technical Reports of the Aeronautical Research Council—

December 1, 1936—June 30, 1939	R. & M. No. 1850	1*s*. 3*d*. (1*s*. 5*d*.)
July 1, 1939—June 30, 1945	R. & M. No. 1950	1*s*. (1*s*. 2*d*.)
July 1, 1945—June 30, 1946	R. & M. No. 2050	1*s*. (1*s*. 2*d*.)
July 1, 1946—December 31, 1946	R. & M. No. 2150	1*s*. 3*d*. (1*s*. 5*d*.)
January 1, 1947—June 30, 1947	R. & M. No. 2250	1*s*. 3*d*. (1*s*. 5*d*.)

Published Reports and Memoranda of the Aeronautical Research Council—

Between Nos. 2251–2349	R. & M. No. 2350	1*s*. 9*d*. (1*s*. 11*d*.)
Between Nos. 2351–2449	R. & M. No. 2450	2*s*. (2*s*. 2*d*.)
Between Nos. 2451–2549	R. & M. No. 2550	2*s*. 6*d*. (2*s*. 10*d*.)
Between Nos. 2551–2649	R. & M. No. 2650	2*s*. 6*d*. (2*s*. 10*d*.)
Between Nos. 2651–2749	R. & M. No. 2750	2*s*. 6*d*. (2*s*. 10*d*.)

Prices in brackets include postage

HER MAJESTY'S STATIONERY OFFICE

York House, Kingsway, London W.C.2; 423 Oxford Street, London W.1; 13a Castle Street, Edinburgh 2; 39 King Street, Manchester 2; 2 Edmund Street, Birmingham 3; 109 St. Mary Street, Cardiff; Tower Lane, Bristol 1; 80 Chichester Street, Belfast, *or through any bookseller.*

S.O. Code No. 23-3115